

Visualization of forward and reflected components in minute vibration velocity waveform of human arterial wall

ヒト動脈壁微小振動速度波形に含まれる進行波・反射波成分の可視化

Kazue Hongo^{1†}, Hideyuki Hasegawa^{1,2} and Hiroshi Kanai^{2,1} (¹ Grad. School of Biomed. Eng., Tohoku Univ.; ² Grad. School of Eng., Tohoku Univ.)
本江和恵^{1†}, 長谷川英之^{1,2}, 金井 浩^{2,1} (¹東北大院 医工; ²東北大院 工)

1. Introduction

The number of patients suffering from atherosclerosis increases rapidly with the development of aging society and westernization of food life. It is important to make an early diagnosis of the atherosclerosis to prevent serious disease such like myocardial and cerebral infarction.

The pulse wave velocity methods are known as a one of the diagnosis method of the atherosclerosis. This method uses pulse wave velocity, which is the velocity of the pressure wave generated by heartbeat and propagates along the longitudinal direction of the artery. Pulse wave velocity c_{PWV} becomes faster with progress of atherosclerosis and can be expressed by the Moens-Korteweg's equation, as follows:

$$c_{PWV} = \sqrt{Eh / \rho D}, \quad (1)$$

where E is the Young's modulus, h is the thickness of the arterial wall, ρ is the blood density, and D is the diameter of artery.

Since the traditional pulse wave velocity is measured between carotid artery and femoral artery, it is not suitable for early diagnosis of atherosclerosis because sizes of lesions of early atherosclerosis are in several millimeters. Thus, measurement of the regional pulse wave velocity is essential for diagnosis of early-stage atherosclerosis.

In this study, the propagation of the pulse wave in the carotid artery of about 14 mm in length was visualized by analyzing the phase of the vibration velocity waves measured at multiple points along the arterial wall in the frequency domain.

2. Method

In this study, minute vibration velocity of the human carotid arterial wall was measured by the phased-tracking method¹⁾ on 72 points along the arterial longitudinal direction with intervals of 0.2 mm.

The average velocity $v(t)$ of an object during the transmission interval ΔT of ultrasound pulses is accurately estimated using the phase shift in the succeeding received ultrasonic pulses, as follows:

$$v(t + \Delta T / 2) = -\frac{c}{2\Delta T} \frac{\Delta\theta_{t+\Delta T/2}(\omega_0)}{\omega_0} \quad (2)$$

where c is the velocity of ultrasound, ω_0 is the center angular frequency, $\Delta\theta_{t+\Delta T/2}(\omega_0)$ is the phase shift of the received ultrasound signal during ΔT .

To realize a high frame rate, parallel beam forming²⁾ was employed. In this method, the number of transmissions was reduced using plane waves in transmission and creating multiple focused receiving beams per transmission. In the present study, the number of transmissions was 3, and 72 receiving beams were obtained for 3 transmissions. The 72 velocity waveforms were analyzed by the discrete Fourier transform to obtain the phase at each frequency.

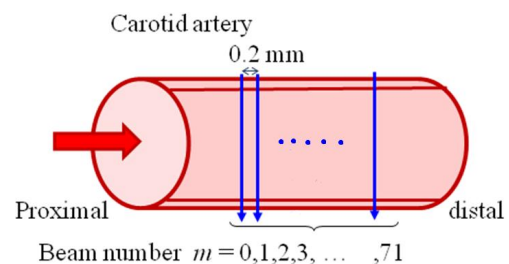


Fig. 1 Method for measuring the minute vibration velocity waveforms of human carotid arterial wall.

Each velocity waveform is composed of a forward component from the heart to the periphery and a reflected component from the periphery to the heart. For detailed analyses of pulse wave, differentiation of each component is important.

In this article, the pulse wave propagation was visualized by mapping phase distribution of velocity waveforms.

3. Result

The minute vibration velocity waveforms of

[†]E-mail address: hongo@us.ecei.tohoku.ac.jp

human arterial wall were measured at 72 points (beam number $m = 0, 1, \dots, 71$) with intervals Δx of 0.2 mm as shown in Fig. 1. The velocity waveforms of beam number $m = 0$ and 71 are shown in Fig. 2.

Before frequency analysis, a Hanning window (window width: 50.1 ms) was applied to each velocity waveform. Frequency spectra were obtained with time intervals of 0.28 ms.

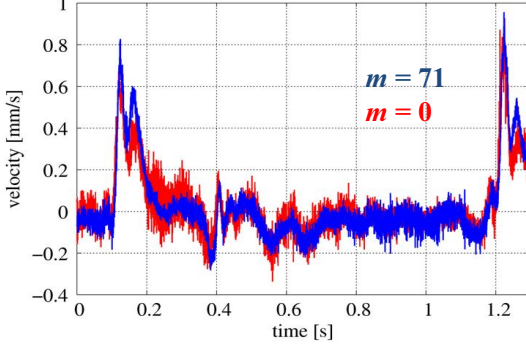


Fig. 2 The minute vibration velocity waveforms of beams 0 and 71.

To visualize forward and reflected components in minute vibration velocity waveform of human arterial wall by phase distribution, negative peaks around $t = 0.34\sim 0.46$ seconds were analyzed.

component is shown using color, horizontal axis is time t [s] and vertical axis shows beam number $m = 0\sim 71$. The specific frequency of 60Hz was determined using the following magnitude-squared coherence function (MSCF) and the power spectra.

$$|\gamma(f)|^2 = \frac{|E_m[Y_m^*(f)Y_{m+1}^*(f)]|^2}{E_m[|Y_m(f)|^2]E_m[|Y_{m+1}(f)|^2]}, \quad (3)$$

where $Y_m(f)$ is the spectrum obtained at beam number m , $E_m[\]$ is average operation for 72 beams. The MSCF $|\gamma(f)|^2$ shows the frequency components which propagate linearly along the artery.

In Figs. 4(a) and 4(b), phases of frequency spectra at 20 Hz and 60 Hz were shown for the negative peak of velocity around 0.38 s and that around 0.425 s, respectively, by the peaks of power spectra and that MSCFs were close to 1. As shown in Fig. 4, the phase of vibration changes during propagation. Using phase $\theta_m(f)$ obtained at beam position m and frequency f , propagation velocity c_{PWV} is determined as follows:

$$c_{PWV} = -2\pi\Delta x \frac{f}{\theta_m(f)} \quad (4)$$

As shown by Eq. (4), c_{PWV} can be obtained by estimating the slope $\theta_m(f)/f$ of the frequency characteristic of the phase. The pulse wave velocities obtained from Figs. 4(a) and 4(b) for the forward and reflected components were 7.0 m/s and

-7.2 m/s, respectively, where the positive velocity corresponds to propagation from the heart to the periphery.

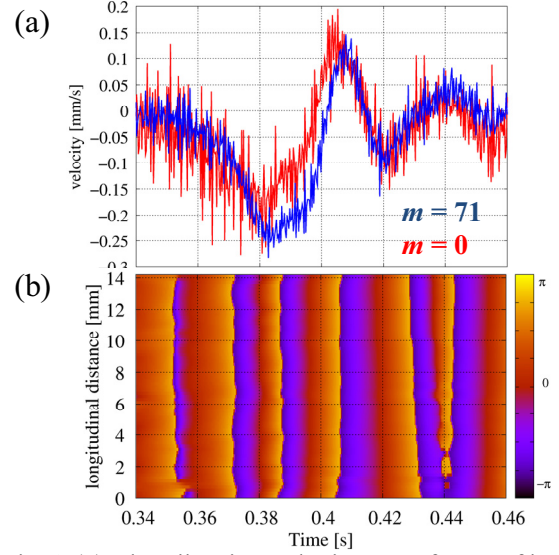


Fig. 3 (a) The vibration velocity waveforms of beam number 0 and 71. (b) The visualization of phase propagation ($f = 60\text{Hz}$).

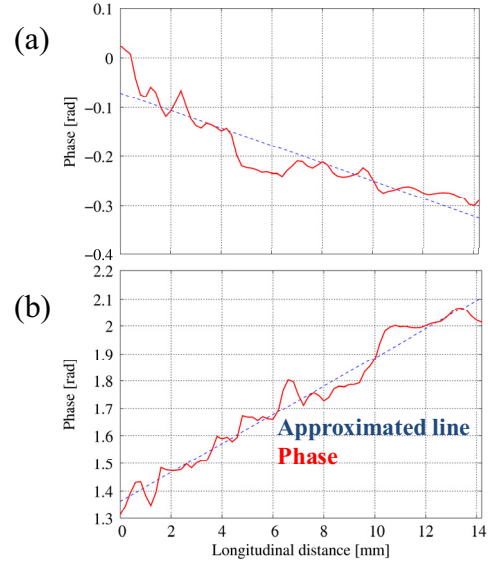


Fig. 4 The phase propagation at the specific time (a) $t = 0.38$ s ($f = 20\text{Hz}$). (b) $t = 0.425$ s ($f = 60\text{Hz}$).

4. Conclusion

In this study, we could differentiate the forward and reflected components in vibration velocity of the carotid arterial wall using the phase spectrum.

References

1. H. Kanai, et al., *IEEE Trans. on UFFC*, **43**, pp.791-810 (1996).
2. Hasegawa and H. Kanai., *IEEE Trans. on UFFC*, **55**, pp. 2626-2639 (2008).